



University of Technology Sydney

**Advanced Control Strategies for Vehicle to Grid
Systems with Electric Vehicles as Distributed Sources**

Yanqing Qu


**School of Electrical, Mechanical and Mechatronic Systems
University of Technology Sydney, Australia**

**A thesis submitted to the University of Technology Sydney
for the Degree of Doctor of Philosophy**

CERTIFICATE OF AUTHORSHIP/ORIGINALITY

I certify that the work in this thesis has not previously been submitted for a degree nor has it been submitted as part of requirements for a degree as fully acknowledged with the text.

I also certify that the thesis has been written by me. Any help that I have received in my research work and the preparation of the thesis itself has been acknowledged. In addition, I certify that all information sources and literature used are indicated in the thesis.


Signature of Candidate

Acknowledgements

First of all, I would like to express heartfelt gratitude and appreciation to my supervisor, Professor Jianguo Zhu, for his enthusiastic help, inspiration, patience, unlimited support and consistent encouragement throughout the entire research period providing the opportunity to work in this highly promising research field. I am also grateful to Associate Professor Youguang Guo, my co-supervisor, for his useful suggestions and encouragement of my attitude.

Also, I would like to thank Professor Guoxiu Wang, the external co-supervisor, from the School of Mathematical and Physical Sciences, Faculty of Science for his precious discussion and comments. His research experience on electrochemical energy storage components has made a significant contribution to the hybrid energy storage system development.

I would also like to express thanks to my research group mates, in particular Dr. Jiefeng Hu and Dr. Gang Lei of the Centre for Electrical Machines and Power Electronics, University of Technology Sydney (UTS), for their precious time, professional advice, sharing of knowledge, technical support and friendship. Their opinions and advices have provided me with great assistance in completing my PhD research work.

On a personal aspect, I would like to thank my parents for their love and support given to me during this research period. Their support is so important for me to finish my PhD study and grow up in Australia. I also would like to thank my special friends who helped me and gave me essential support during this period of study.

TABLE OF CONTENTS

CERTIFICATE OF AUTHORSHIP/ORIGINALITY	i
ACKNOWLEDGEMENTS	ii
TABLE OF CONTENTS	iii
LIST OF SYMBOLS	vii
LIST OF ABBREVIATIONS	xi
LIST OF FIGURES	xiv
LIST OF TABLES	xix
ABSTRACT	xx
1. INTRODUCTION	1
1.1 Background and Significance	1
1.2 Development of Electric Vehicles	3
1.3 The Concept of V2G Services	5
1.4 Smart Car Parks in Power Grids	7
1.5 Research Objectives	10
1.6 Outline of the Thesis	12
References	13
2. LITERATURE SURVEY	19
2.1 Introduction	19
2.2 Vehicles and Energy Sources	19
2.3 Battery Charging and Grid Connection	26
2.4 V2G System Requirements and Power Flow	28
2.5 Smart Charging	36

2.6 EV-Grid Models	37
2.7 Control Algorithm for Bidirectional Power Flow	41
2.7.1 Voltage oriented control	41
2.7.2 Direct control	42
2.7.3 Space vector modulation direct control	42
2.7.4 Model predictive control	43
2.8 Grid Support from V2G Services	45
2.8.1 Load balancing and peak power (load management)	46
2.8.2 Support to systems containing renewable energy resources	47
2.8.3 Electric grid interaction for grid support	47
2.9 Economic Issues Related to V2G Services	49
2.10 Summary of the Chapter	55
References	56
3. ENERGY STORAGE SYSTEM FOR ELECTRIC VEHICLES	73
3.1 Introduction	73
3.2 Model Development of Batteries as Energy Storage System in EVs	75
3.2.1 Battery characteristics for model development	75
3.2.2 Battery model development procedure	79
3.3 Model Development of Supercapacitors as Energy Storage System in EVs	81
3.3.1 Supercapacitor characteristics for model development	81
3.3.2 Supercapacitor model parameter calculation	84
3.4 Balancing Circuit Development for Energy Storage System	89
3.4.1 Supercapacitor cell voltage balancing necessity	91
3.4.2 Equalization scheme types	92
3.4.3 Supercapacitor cell voltage balancing methods comparison	93
3.4.4 Novel balancing circuit development for supercapacitor storage bank	99
3.5 Numerical Simulations and Experimental Verifications	108
3.5.1 Supercapacitor experimental test	108
3.5.2 Battery experimental test	122
3.5.3 Test performance of supercapacitor cell balancer	136
3.6 Summary of the Chapter	141

References	142
4 IMPLEMENTATION OF THE V2G SYSTEM AT COMPONENT LEVEL	148
4.1 Introduction	148
4.2 Direct Power Control for Bidirectional Power Flow Control	151
4.3 Model Predictive Control for Bidirectional Power Flow Control	154
4.4 Flexible Power Regulation between Grid and EVs	156
4.5 Numerical Simulation	160
4.5.1 Comparison between MPC and conventional DPC	160
4.5.2 Bidirectional power flow control	165
4.6 Summary of the Chapter	168
References	169
5 GRID SUPPORT FROM V2G SERVICES	175
5.1 Introduction	175
5.2 Modelling of Bidirectional Charger Used for V2G Support to Grid	181
5.3 Aggregator Development of V2G services	183
5.4 V2G Service for Grid Stability from EV Parks	190
5.4.1 Power system and V2G system modelling in the PSCAD/EMTDC	191
5.4.2 Power compensation from EVs to the grid	194
5.5 Simulation Results and Scaled Down Experimental Test Results for V2G Service	202
5.5.1 Experimental results of the generator performance when load changes	205
5.5.2 Simulation results of the V2G support to power system when load changes	207
5.6 Summary of the Chapter	208
References	209
6 ECONOMIC ISSUES RELATED TO V2G SERVICES	212
6.1 Introduction	212

6.2 V2G System Information Collection for SmartPark	213
6.2.1 EVs information collection	214
6.2.2 Grid side information collection	218
6.3 Optimal Charging Based on Different Objectives	226
6.3.1 As fast as possible charging (AFAP)	226
6.3.2 Maximization of the average state of charge (SOC) for all vehicles at the next time step	229
6.3.3 Maximum revenue static charging scheduling problem (R-SCSP) and Minimum cost dynamic charging scheduling problem (C-DCSP)	232
6.4 Summary of the Chapter	237
References	238
7 CONCLUSIONS AND FUTURE WORK	240
7.1 Conclusions	240
7.2 Future work	241
APPENDIX. PUBLICATIONS BASED ON THE THESIS PROJECT	242

List of Symbols

A	Normal distribution of arrival time
$A0, A1, A2$	Control of address signals
a	Regulation prices [\$]
B	Cost upper bound [\$]
$C, C_{1c}, C_{2c}, C_{3c}, C_{4c}$	Capacitor capacitance [F]
$Cap_{r,i}(k)$	Remaining battery capacity needed to be filled [F]
$C_{i,t}$	Cost of charging EV i at timeslot t (\$)
D	Normal distribution of departure time
$d_P d_Q$	Digitized signals by two fixed-band hysteresis comparators
d_t	Energy consumption at time t (Wh)
E	Energy density (Wh/L)
e	Line to line AC Voltage (V)
f	Source voltage frequency (hZ)
g	Electricity prices (\$)
I	Current supplied by the battery (A)
$I_1(t)$	Current value across supercapacitor (A)
I_a	Charger current (A)
I_C	Charge current across R_{1c} (A)
K_f	Infrastructure cost (\$)
K_{T1}	Transformer T1 ratio
K_{T2}	Transformer T2 ratio
K_{T3}	Transformer T3 ratio
l	Base loads (W)
M	Estimated number of miles driven daily (km)
$m_{i,t}$	Aggregator's revenue from EV i at timeslot t (\$)

N	Total number of plug-in electric vehicles (PEVs)
P	Active power exchanged with the grid (W)
P_{EV}	Charging station injects active power (W)
P_{EVavg}	Average constant power requirement for all PEVs (W)
P_i	Active power flows in line i (W)
$p_{i,t}$	Charging rate of EV i at timeslot t (kW)
$\bar{P}_{i,t}$	Maximum charging rate limit of EV i at timeslot t (kW)
P_{Li}	Active load at bus i (W)
P_{ref}	Active power reference (W)
P_t	Price per energy unit at time t (\$)
Q	Reactive power exchanged with the grid (Var)
Q_{EV}	Charging station injects reactive power (Var)
Q_i	Reactive power flows in line i (Var)
Q_{Li}	Reactive load at bus i (Var)
Q_{ref}	Reactive power reference (Var)
R	Transformer delivery capacity (W)
R_0	Series resistor of battery (Ω)
R_l	Parallel resistor of battery (Ω)
$R_{1c}, R_{2c}, R_{3c}, R_{4c}$	Resistor (Ω)
R_L	Leakage resistor of supercapacitor (Ω)
R_S	Series resistor of supercapacitor (Ω)
$r_{i,t}$	Regulation capacity of EV i at timeslot t (kW)
$S_{a1}-S_{a5} S_{b1}-S_{b5}$	Bidirectional switches
S_B	System rated power (W)
S_{EV}	Power supplied by the battery (W)
SOC_{end}	Terminal EV battery SOC
SOC_{init}	Initial EV battery SOC

SOC_{max}	Maximum storage capacity (Ah)
SOC_t	SOC level for at time t
T	Total number of timeslots
$T_{r,i}(k)$	Remaining time for charging the i th vehicle at time step k
T_s	Sample time
U_B	System rated voltage (V)
$U^*(t)$	Voltage value of supercapacitor (V)
V	Voltage of voltage source (V)
$V_1 \sim V_5, V_6 \sim V_{11}$	Terminal voltage (V)
V_a	Grid voltage (V)
V_b	Voltage present voltage (V)
V_b^*	Reference battery voltage (V)
$V_{b,nom}$	Voltage nominal value (V)
V_{dc}	DC bus voltage (V)
V_E	Terminal voltage of capacitor C_{1c} (V)
V_i	Voltage of bus i (V)
V_{oc}	Open-circuit voltage (V)
V_s	Terminal voltage for supercapacitor before charge (V)
ΔV_o	Jump of terminal voltage across capacitor (V)
X	Line reactance between the converter and the utility node (Ω)
$x_{i,t}$	SOC of EV i at time t
Z_t	Location of the EV at time t
Δ	Angle between E and V
λ_t	V2G parameter for at time t
η_c	Charging efficiency
η_d	Discharging efficiency
Ψ_e	Energy-related battery degradation cost (\$/kWh)

Ψ_p	Power-related battery degradation cost (\$/kWh ²)
ϕ	Net charging amount (kWh)
φ_t	Charge parameter for at time t (kWh)
Φ_i	Charging schedule for a given charging task i
$\bar{\varphi}$	Maximum charging amount per time slot (kWh)
$\psi_e \varphi_t$	Line term reflecting the degradation from energy throughput
$\psi_p \varphi_t^2$	Quadratic term reflecting power-related degradation

List of Abbreviations

ACE	Area Control Error
AFAP	As Fast as Possible Charging
AGC	Automatic Generation Control
BESS	Battery Energy Storage System
BEV	Battery Electric Vehicle
BMS	Battery Management System
C-DCSP	Cost Dynamic Charging Scheduling Problem
CNT	Carbon NanoTube
CVT	Continuously Variable Transmission
DER	Distributed Energy Resource
DOD	Depth of Discharge
DPC	Direct Power Control
DSO	Distribution System Operator
DTC	Direct Torque Control
EIS	Electrochemical Impedance Spectroscopy
EMI	Electromagnetic Interference
EMTDC	Electromagnetic Transient and DC
EPA	Environmental Protection Agency
EPRI	Electric Power Research Institute
ESP	Energy Service Provider
EV	Electrical Vehicle
FACTS	Flexible AC Transmission System
FCV	Fuel Cell Vehicle
GV	Grid-able Vehicle
G2V	Grid to Vehicle
HEV	Hybrid Electrical Vehicle
HVDC	High Voltage Direct Current
ICE	Internal Combustions Engine

IGBT	Insulated-gate Bipolar Transistor
IGCT	Integrated-gate Commutated Thyristor
ISO	Independent System Operator
LP	Linear Programming
MPC	Model Predictive Control
NEC	National Electrical Code
NERC	National Electric Reliability Council
OCV	Open Circuit Voltage
PEM	Proton Exchange Membrane
PEV	Plug-in Electric Vehicle
PFCV	Plug-in Fuel Cell Vehicle
PHEV	Plug-in Hybrid Electrical Vehicle
PI	Proportional-integral
PLC	Power Line Communication
PSO	Particle Swarm Optimization
PSCAD	Power System Computer Aided Design
PV	Photovoltaic
PWM	Pulse Width Modulation
R-DCSP	Revenue Dynamic Charging Scheduling Problem
RES	Renewable Energy Resources
R-SCSP	Revenue Static Charging Scheduling Problem
SCs	Supercapacitors
SDPC	Switching Table-based Direct Power Control
SGSS	Smart Grid Stabilization System
SMPS	Switched Mode Power Supply
SOC	State of Charge
STATCOM	Static Compensator
SVM	Space Vector Modulator
V2B	Vehicle to Building
VFC	Voltage to Frequency Converters

V2G	Vehicle to Grid
V2I	Vehicle to Infrastructure
VOC	Voltage Oriented Control
VSI	Voltage Source Inverter
V2X	Vehicle to any Load
WSCC	Western System Coordinating Council

LIST OF FIGURES

- Fig. 1.1 Overview of the proposed PEVs network charging system with renewable resources
- Fig. 1.2 Typical structure of a parking lot for V2G system
- Fig. 2.1 Typical EV configuration
- Fig. 2.2 Toyota Prius configuration (a) HEV, (b) converted PHEV
- Fig. 2.3 Fuel cell vehicle configuration (a) FCV, (b) PFCV
- Fig. 2.4 Typical variable-speed electric motor characteristics
- Fig. 2.5 Typical electric motor efficiency characteristics
- Fig. 2.6 Components and power flow of a V2G system
- Fig. 2.7 EV power electronics configuration with V2G
- Fig. 2.8 AC propulsion V2G model AC-150 (a) electrical schematic, (b) picture of the package
- Fig. 2.9 Single-stage power electronics topologies with (a) Single-phase inverter; (b) Three-phase inverter
- Fig. 2.10 Cascaded power electronic topologies with DC-DC and DC-AC converters
- Fig. 2.11 Bidirectional isolated DC-DC power electronics topology
- Fig. 2.12 Generalized power electronics and control of a battery energy storage system
- Fig. 2.13 Block diagram of VOC
- Fig. 2.14 Block diagram of DPC
- Fig. 2.15 Block diagram of SVM-DPC
- Fig. 2.16 Block diagram of model predictive control
- Fig. 2.17 Envisioned large-scale PHEV/PEV charging/V2G infrastructure in a smart grid environment
- Fig. 2.18 EV charging configuration at AC level 1 and 2 setup (i.e. on-board charger).
- Fig. 2.19 EV charging configuration at DC level 1 and 2 framework (i.e. off-board charger)
- Fig. 2.20 The power output and battery state of charge for an electric vehicle providing frequency regulation ancillary service
- Fig. 3.1 Indicative Ragone plots for different energy storage devices
- Fig. 3.2 Schematic representation of operation of electrochemical cell. (a) Discharge (b) Charge
- Fig. 3.3 Typical battery discharge curve
- Fig. 3.4 Circuit-oriented battery models (a), (b) and (c)
- Fig. 3.5 First-order Thevenin charging model
- Fig. 3.6 Double layer capacitor
- Fig. 3.7 Three layer supercapacitor structure
- Fig. 3.8 Model of supercapacitor used
- Fig. 3.9 EIS Nyquist plot of supercapacitor
- Fig. 3.10 Simplest electric model
- Fig. 3.11 Equivalent charge circuit model
- Fig. 3.12 Cell equalization circuit using switched resistor

- Fig. 3.13 (a) Typical flyback-converter-based equalize, (b) Inductor coupling flyback-converter-based equalizer, (c) Buck-boost-based modular current divider
- Fig. 3.14 Equalization using MOSFET to achieve the balancing
- Fig. 3.15 Equivalent circuit of the proposed cell voltage equalizer: (a) state 1: Sa is ON and Sb is OFF, (b) state 2: Sa is OFF and Sb is ON
- Fig. 3.16 Bidirectional switch
- Fig. 3.17 Circuit diagram of cell balancing circuit using Switched capacitor based on the Cockcroft-Walton scheme
- Fig. 3.18 Simulation results of the voltage waveform using switched capacitor based on the Cockcroft-Walton scheme
- Fig. 3.19 Switchless cell voltage equalizer
- Fig. 3.20 Current flow direction in (a) mode A and (b) mode B
- Fig. 3.21 Circuit diagram of cell balancing circuit using switchless voltage equalizer
- Fig. 3.22 Simulation results of the voltage waveform using switchless voltage equalizer
- Fig. 3.23 Circuit diagram of cell balancing circuit using transformer
- Fig. 3.24 Simulation results of the voltage waveform using transformer
- Fig. 3.25 Energy recovery for a capacitor versus depth of discharge
- Fig. 3.26 Voltage monitoring circuit diagram
- Fig. 3.27 Cell balancer diagram
- Fig. 3.28 Cell Balancer SMPS and VFC
- Fig. 3.29 Local controller with dummy VFC Controller plugged into J32
- Fig. 3.30 Front panel LED display
- Fig. 3.31 Supercapacitor from Jinzhou Kaimei Power Co.
- Fig. 3.32 The charge circuit for supercapacitor
- Fig. 3.33 The self-discharge circuit for supercapacitor
- Fig. 3.34 1.96 Ω load discharge circuit
- Fig. 3.35 Power supply used to charge the supercapacitor
- Fig. 3.36 Power supply used for current sensor board from NI
- Fig. 3.37 Current sensor used to transfer current signal to voltage signal
- Fig. 3.38 DAQ board used to collect the voltage data of supercapacitor and current sensor
- Fig. 3.39 Supercapacitor connected into the circuit
- Fig. 3.40 The waveform view of Labview
- Fig. 3.41 The blocks of Labview to collect data
- Fig. 3.42 The whole work station
- Fig. 3.43 Voltage of No.1 supercapacitor for self-discharge
- Fig. 3.44 Voltage of No.2 supercapacitor for self-discharge
- Fig. 3.45 Voltage of No.3 supercapacitor for self-discharge
- Fig. 3.46 Voltage of No. 1 supercapacitor for 3.15A constant charging
- Fig. 3.47 Voltage of No. 2 supercapacitor for 3.15A constant charging
- Fig. 3.48 Voltage of No. 3 supercapacitor for 3.15A constant charging
- Fig. 3.49 Voltage of No.1 supercapacitor for 1.96 Ω load discharge
- Fig. 3.50 Voltage of No.2 supercapacitor for 1.96 Ω load discharge

- Fig. 3.51 Voltage of No.3 supercapacitor for 1.96 Ω load discharge
- Fig. 3.52 No.1 supercapacitor recovery performance
- Fig. 3.53 No.2 supercapacitor recovery performance
- Fig. 3.54 No.3 supercapacitor recovery performance
- Fig. 3.55 Basic model voltage curve comparison with experiment results
- Fig. 3.56 Voltage error between model and experiment
- Fig. 3.57 Simulink block diagram of supercapacitor model charging
- Fig. 3.58 Constant current charging with 3.15A for 91 seconds
- Fig. 3.59 Voltage of supercapacitor during constant current charging procedure
- Fig. 3.60 Comparison of the experimental and simulation results
- Fig. 3.61 Nanophosphate battery from A123 company
- Fig. 3.62 Schematic illustration of the Nanophosphate structure, with secondary and primary particles
- Fig. 3.63 2A constant current charge for the No. 1 battery
- Fig. 3.64 3A constant current charge for the No. 1 battery
- Fig. 3.65 4A constant current charge for the No. 1 battery
- Fig. 3.66 Comparison of different current charge for the No. 1 battery
- Fig. 3.67 2A constant current charge for the No. 2 battery
- Fig. 3.68 3A constant current charge for the No. 2 battery
- Fig. 3.69 4A constant current charge for the No. 2 battery
- Fig. 3.70 Comparison of different current charge for the No. 2 battery
- Fig. 3.71 3A constant current charge for the No. 3 battery
- Fig. 3.72 4A constant current charge for the No. 3 battery
- Fig. 3.73 Experimental setup for measuring battery charge performance
- Fig. 3.74 First-order Thevenin charging model
- Fig. 3.75 Experiment results of charging behaviour
- Fig. 3.76 Curve fitting of $[U_t(t)-U_{oc}]$ versus time (starting SOC=0%)
- Fig. 3.77 Curve fitting of $[U_t(t)-U_{oc}]$ versus time (starting SOC=10%)
- Fig. 3.78 Curve fitting of $[U_t(t)-U_{oc}]$ versus time (starting SOC=20%)
- Fig. 3.79 Curve fitting of $[U_t(t)-U_{oc}]$ versus time (starting SOC=30%)
- Fig. 3.80 Curve fitting of $[U_t(t)-U_{oc}]$ versus time (starting SOC=40%)
- Fig. 3.81 Curve fitting of $[U_t(t)-U_{oc}]$ versus time (starting SOC=50%)
- Fig. 3.82 Curve fitting of $[U_t(t)-U_{oc}]$ versus time (starting SOC=60%)
- Fig. 3.83 Curve fitting of $[U_t(t)-U_{oc}]$ versus time (starting SOC=70%)
- Fig. 3.84 R_0 variation with different SOC starting
- Fig. 3.85 R_1 variation with different SOC starting
- Fig. 3.86 A single supercapacitor module
- Fig. 3.87 Three supercapacitor modules in test bed
- Fig. 3.88 Input power and efficiency versus cell voltage
- Fig. 3.89 VFC output frequency versus cell voltage using a 250 kHz VFC clock
- Fig. 4.1 V2G charger structure with the AC transmission bus
- Fig. 4.2 Three-phase AC-DC converter topology

- Fig. 4.3 control block of SDPC
- Fig. 4.4 possible voltage vectors
- Fig. 4.5 Control block of model predictive control (MPC)
- Fig. 4.6 Four quadrant operation of power flow through inverter between grid and vehicle
- Fig. 4.7 Branch of a radial distribution system
- Fig. 4.8 Input AC side V_a and I_a (DPC)
- Fig. 4.9 Input AC side V_a and I_a (DPC) (0.15s-0.25s)
- Fig. 4.10 Input I_a , I_b and I_c (DPC)
- Fig. 4.11 Input I_a , I_b and I_c (DPC) (0.15s-0.25s)
- Fig. 4.12 Output DC voltage V_{dc} (DPC)
- Fig. 4.13 Input active power P (DPC)
- Fig. 4.14 Input reactive power Q (DPC)
- Fig. 4.15 Input AC side V_a and I_a (MPC)
- Fig. 4.16 Input AC side V_a and I_a (MPC) (0.15s-0.25s)
- Fig. 4.17 Input I_a , I_b and I_c (MPC)
- Fig. 4.18 Input I_a , I_b and I_c (MPC) (0.15s-0.25s)
- Fig. 4.19 Output DC voltage V_{dc} (MPC)
- Fig. 4.20 Input active power P (MPC)
- Fig. 4.21 Input reactive power Q (MPC)
- Fig. 4.22 Three-phase bidirectional AC-DC converter topology used in V2G system
- Fig. 4.23 Active power P and reactive power Q in one chart
- Fig. 4.24 Grid voltage V_a (1/10 scaled) and charger current I_a , waveforms for each operation mode. (a) Mode#1-discharging operation. (b) Mode#2-discharging and capacitive operation. (c) Mode#3-charging operation. (d) Mode#4-charging and inductive operation.
- Fig. 5.1 Illustrative schematic of power line and wireless control connections between vehicles and the electric power grid
- Fig. 5.2 A single container of A123's Smart Grid Stabilization System (SGSS)
- Fig. 5.3 Power electronics-interfaced EV applications in the power grid
- Fig. 5.4 EVs batteries used as a distributed energy source
- Fig. 5.5 Aggregator in V2G system
- Fig. 5.6 Computer/communication/control network for the framework of V2G system
- Fig. 5.7 Classification of power system stability
- Fig. 5.8 3 generators, 9 buses power system from WSCC
- Fig. 5.9 3 generators, 9 buses power system model block diagram in PSCAD/EMTDC
- Fig. 5.10 V2G system model block diagram in PSCAD/EMTDC
- Fig. 5.11 Frequency recovery performance comparison. (a) Without EVs' active power compensation. (b) With EVs' active power compensation
- Fig. 5.12 Voltage recovery performance at bus 4 (Increase reactive load at bus 4 and use EVs to compensate the reactive power at 4s)

- Fig. 5.13 Different buses voltage variation when there is reactive load change at bus 4 and reactive power from EVs compensated at bus 4. (a) Bus 4. (b) Bus 1. (c) Bus 2. (d) Bus 3. (e) Bus 5. (f) Bus 6.
- Fig. 5.14 Voltage change comparison results among different bus numbers when there is reactive power load change at bus 4 and reactive power from EVs compensated at bus 4
- Fig. 5.15 Connection of transformer and load
- Fig. 5.16 Display and control panels of Easygen-3000 in the laboratory
- Fig. 5.17 PT screen
- Fig. 5.18 Experimental test bed for the generator when load changes
- Fig. 5.19 Output voltage waveform of resistor load without V2G support
- Fig. 5.20 Output voltage waveform of resistor and capacitive load without V2G support
- Fig. 5.21 Output voltage waveform of resistor, capacitive and inductive load without V2G support
- Fig. 5.22 V2G support to power system when load changes
- Fig. 6.1 The probability density function of arrival time A
- Fig. 6.2 The probability density function of arrival time D
- Fig. 6.3 The probability density function of parking time
- Fig. 6.4 Average kilometres travelled, Motor vehicles by state/territory of registration Year ended 30 June 2012
- Fig. 6.5 The probability density function of the daily travel distance
- Fig. 6.6 System load following and regulation
- Fig. 6.7 Electricity load demand data in a typical day in NSW (11/3/2015)
- Fig. 6.8 Load curve and load following line in a typical day in NSW (11/3/2015)
- Fig. 6.9 Power regulation pattern in a typical day in NSW (11/3/2015)
- Fig. 6.10 Electricity load demand data in a typical month in NSW (1/12/2014-31/12/2014)
- Fig. 6.11 Electricity load demand data in a typical month in NSW 24 hours a day 31 days a month (1/12/2014-31/12/2014)
- Fig. 6.12 Electricity price variation in a typical month in NSW (1/12/2014-31/12/2014)
- Fig. 6.13 Electricity price variation in a typical month in NSW 24 hours a day 31 days a month (1/12/2014-31/12/2014)
- Fig. 6.14 The illustration of the remaining battery capacity

LIST OF TABLES

TABLE 2.1 AC/DC Charging Levels Characteristics as per SAE J1772 Standard

TABLE 2.2 Mathematical Model Formulation of V2G Optimization

TABLE 3.1 2005 Comparison of Energy Density of Various Energy Storage Technologies

TABLE 3.2 Extraction Results of R_o and R_1

TABLE 4.1 Switching Table of Conventional SDPC

TABLE 4.2 Electrical Parameters of Power Circuit

TABLE 4.3 Electrical Parameter of Power Circuit

TABLE 4.4 Battery Parameters Block Used in the Simulink

TABLE 4.5 Two V2G Mode Worked in the Simulation

TABLE 5.1 Key Features about a Single Container of A123's Smart Grid Stabilization System

TABLE 5.2 Model Parameters of a 3 Generator, 9 Bus Power System Model

TABLE 6.1 Parameters for PEVs in Different Sizes

TABLE 6.2 Average Distance and Electricity Consumption for a Typical PHEV

TABLE 6.3 Total Energy Available For Grid Support

TABLE 6.4 Total Energy Available For Grid Support

TABLE 6.5 Total Energy Required During Charging

TABLE 6.6 Total Energy Required During Charging

TABLE 6.7 Model Parameters

TABLE 6.8 The Symbols and Major Notations

ABSTRACT

This thesis focuses on the control and implementation of the vehicle to grid (V2G) system in a smart grid. Important issues like structure, principle, performance, and control of energy storage systems for electrical vehicles and power systems are discussed.

In recent decades, due to rapid consumption of the earth's oil resources, air pollution and global warming (a result of the "greenhouse effect"), the development of electrical vehicles (EVs), hybrid electrical vehicles (HEVs) and plug-in electric vehicles (PEVs) are attracting more and more attentions. In order to provide regulation services and spinning reserves (to meet sudden demands for power), V2G services have a promising prospective future for grid support. It has been proposed that in the future development, such use of V2G could buffer and support effectively the penetration of renewable sources in power systems. This PhD thesis project aims to develop novel and competitive control strategies for V2G services implementation for EVs in smart electrical car parks or Smartparks.

Through a comprehensive literature review of the current EV development and energy storage systems used for EVs, several energy storage technologies are compared and a hybrid energy storage system consisting of batteries and supercapacitors is proposed. This system combines effectively the advantages of high energy density of battery banks and high power density of supercapacitor banks. Supercapacitor and battery cells are tested in the laboratory using different charging and discharging procedures. Different supercapacitor and battery models are compared, discussed, and verified using the experimental data. For the energy storage system package, a cell voltage balance circuit is developed for the supercapacitor module. The principle of this circuit is also applicable to the battery module. The proposed balancing method is simple and reliable, and presents good performance for voltage balancing to prolong the lifetime of the energy storage system.

The essential technology of V2G is based on the bidirectional power flow control of the charger. Besides charging the EV batteries, it can utilize the stored energy to feed electricity back to the power grid when there is a need. Three-phase AC/DC converters have been extensively used in industrial applications and also the V2G chargers. The power converters used for the V2G services are required to operate more efficiently and effectively to maintain high power quality and dynamic stability. Then the AC/DC

converter used for the bidirectional V2G charger is developed and modelled. For the control aspect of AC/DC converter, a new control approach using a model predictive control (MPC) scheme is developed for V2G applications. With the advanced control strategy, the EVs in Smartparks can exchange both active and reactive power with the grid flexibly. The MPC algorithm presents excellent steady-state and dynamic performance.

When a very large number of EVs are aggregated in Smartparks, the charging and discharging power should be a significant viable contributor to the power grid. New challenges will be introduced into the power system planning and operation. While discharging, the V2G power brings more potential benefits to enhance the power quality and system reliability. Using V2G services, EVs can provide many grid services, such as regulation and spinning reserve, load levelling, serving as external storage for renewable sources. An effective approach to deal with the negligibly small impact of a single EV is to group a large number of EVs. An aggregator is a new player whose role is to collect the EVs by attracting and retaining them so as to result in a MW capacity that can beneficially impact the grid. From the aggregator' decision, the EVs are determined by the optimal deployment. The aggregator can act as a very effective resource by helping the operator to supply both capacity and energy services to the grid. By supplying active power and reactive power from EVs, the aggregation may be used for frequency and voltage regulation to control frequency and voltage fluctuations that are caused by supply–demand imbalances. Different case studies of EVs' support to grid are carried out; the results show that V2G services can stabilize the frequency and voltage variations and have control flexibilities to fulfil system reliability and power quality requirements.

The main attractiveness of V2G to consumers is that it can produce income to the vehicle owner to maximize car use. On the other hand, the utility companies can use EVs to stabilize the frequency in the power system and improve the utility operation. It also makes the utility companies more efficient with less loss because the energy is generated locally. From this point of view, V2G is a source of revenue in both electricity and transportation system, and it can help the environment reduce pollution and global warming. Various data of V2G systems have been collected for economic analysis, such as EV battery capacities, charging time, and grid electricity price and load demands. Then for the economic issues related to V2G services, optimal charging based on different objectives is presented. Dumbing charging, maximization of the average state of charge (SOC), maximum revenue and minimum cost are compared. Economic

issues are a very special aspect of the V2G technology and how a large profit from V2G services can be produced is the main point of attraction to vehicle owners.

Significant conclusions based on the research findings are drawn, and possible future works for further development including commercialisation of the V2G technology are proposed.